Received October 16, 2018, accepted November 5, 2018, date of publication November 12, 2018,
date of current version December 7, 2018.

Digital Object Identifier 10.1109/ACCESS.2018.2880456

A Highly Reproducible Fabrication Process for Large-Area Plasmonic Filters for Optical Applications

YUN SEON DO
School of Electronics Engineering, Kyungpook National University, Daegu 41566, South Korea
e-mail: yuns.do@knu.ac.kr

This work was supported in part by the Basic Science Research Program, through the National Research Foundation of Korea (NRF), Ministry of Education, under Grant NRF-2018R1D1A1B07045853, and in part by the Nano·Material Technology Development Program, through NRF, Ministry of Science, ICT and Future Planning, under Grant 2009-0082580.
This paper has supplementary downloadable material available at http://ieeexplore.ieee.org, provided by the author.

ABSTRACT Plasmonic filters are advantageous for fabricating the state-of-the-art color filters without any coloring resist materials. In this paper, a filter design is introduced for the optical structure of plasmonic filters and their fabrication, which allows highly reproducible nanopatterning on large areas. The optical structure of these plasmonic filters consists of 2-D hole arrays in a thin metal film. Although laser interference lithography technology allows a high accuracy of regularity across the whole fabrication region, the exposure light is easily disturbed by vibrations or dust in the air. The suggested process enhances the accuracy and reproducibility of nanopatterns, which also exhibit a high performance. This paper will help realize plasmonic filters in conjunction with industry.

INDEX TERMS Laser interference lithography, nano patterning, surface plasmon, plasmonic filter.

I. INTRODUCTION

Since the discovery by T. W. Ebbessen and his research group in 1998 [1], researchers have been at great efforts to figure out the exact mechanism of the extremely high transmission rate from nanoscale metal openings [2]–[5]. This phenomenon is called ''extraordinary optical transmission (EOT)'' because of the high transmission rates compared to the classical diffraction theory from Bethe [6]. It has been revealed that the main cause of EOT can be attributed to surface plasmons (SPs), which are a collective oscillation movements of free electrons on the metal surface. The spectral transmission of a metallic nano aperture shows high transmittance in the wavelength range of SP resonance. Thus, many research studies have analyzed various types of plasmonic filters (PFs) containing metallic nano apertures for selective spectral filtering, especially in the optical range, i.e., light in the visible to infrared range, and electromagnetic waves in terahertz [7]–[10].

When EOT appears in the visible range, it can be applicable to a color filter which is a key component in enhancing the optical performance of electrical imaging devices, such as displays and CMOS imaging sensors. Compared to conventional color filters, which are based on organic or inorganic color resist materials, PFs show better stability to heat and chemical action as well as high-energy light (e.g., ultraviolet radiation). The thickness of a PF is in the range of hundreds of nanometers and surface plasmons strongly confine the light within a tiny volume. Thus, PFs produce a high value of the density of states of photons. Structures confining large amounts of light in a thin film are of advantage in flexible or transparent devices. In addition, as they include metals in their composition, PFs also exhibit high conductivity and hence can be applied in electrical devices. In this regard, nano apertures in a metal film are preferred to nano metal islands (or particles), which also accompany SPs because of the continuous media.

Our research group previously reported PFs based on two-dimensional (2D) hole arrays in a metal film – a design method with a symmetry-broken structure for practical use [11], [12]. Further, a large-area fabrication process was proposed on the basis of the laser interference lithography (LIL) method [13] and the electrical applications of PFs integrated with transparent thin film transistors [14] and chromatic electrodes [15] were described. The LIL technology is attractive for constructing periodic nano patterns across a large area because the interference pattern produced

2169-3536 © 2018 IEEE. Translations and content mining are permitted for academic research only.
Personal use is also permitted, but republication/redistribution requires IEEE permission.
See http://www.ieee.org/publications_standards/publications/rights/index.html for more information.

by multiple beams provides a regular periodicity. However, the fabricated PFs exhibit a poor uniformity of hole patterns across the entire area; this in turn led to a degradation in their performance.

In this study, a new fabrication process is proposed to achieve higher pattern accuracy and consequently a good PF performance. The suggested process also results in a high reproducibility. This work will allow the practical use of nano structure-based applications.

II. OPTICAL DESIGN OF PLASMONIC COLOR FILTERS

Fig. 1(a) represents the structure of the PF-R which passes the red light between 600 nm to 700 nm. On a glass substrate, a thin aluminum (Al) layer was deposited; it was two dimensionally perforated by circular holes. The array has a square periodicity. Isotropy in periodicity in both the horizontal and vertical directions as well as in the shape of the holes provides independence in the polarization state of the incident light. On top of the Al layer, a lithium fluoride (LiF) film was overlaid.

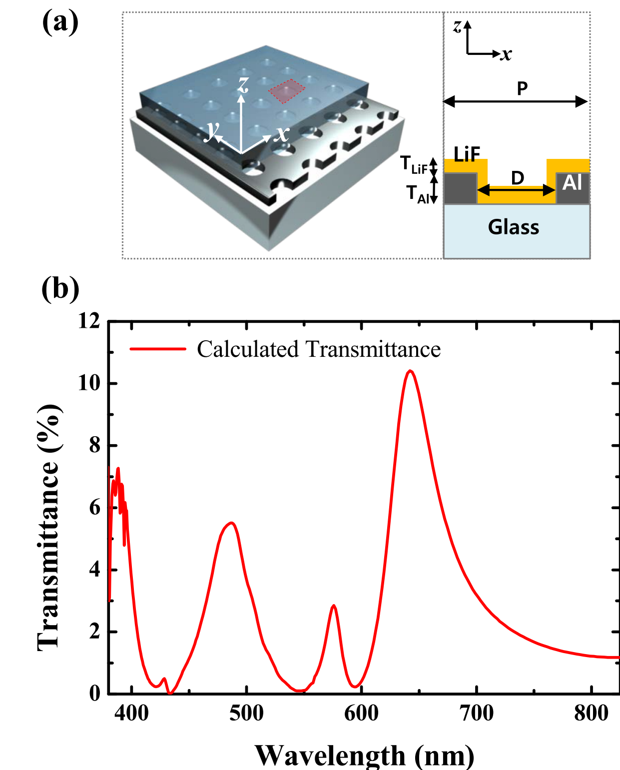

FIGURE 1. (a) Schematic illustration of the plasmonic filter; the dimensions of the structure are shown in the cross-sectional image. (b) The calculated spectral response of the plasmonic filter.

The wavelength of maximum transmittance (λ_{max}) originating from SP resonance is affected by the surrounding dielectric media, as described in (1) [16].

$$\lambda_{max(i,j)} = \frac{P}{\sqrt{i^2 + j^2}} \sqrt{\frac{\varepsilon_m \varepsilon_d}{\varepsilon_m + \varepsilon_d}} \quad (1)$$

Here, P is the period of the hole array, (i,j) is the periodic order in a square array, and ε_m and ε_d are permittivity values of the metal and dielectric material, respectively. A lower energy of light induces more frequent interactions between electromagnetic oscillations [17]. Thus, the highest transmittance generally occurs in the largest wavelength region and originates from the first order of resonance in (1).

Meanwhile, the Al film follows two different SP modes, which are enhanced at the top and bottom surfaces. Thus, the transmittance of the PF can be attributed to the combination of the two SP modes. For the greatest enhancement in SP resonance at a certain wavelength (the target filtering band, λ_{max}), each SP mode should be generated at λ_{max}; this situation is called a "matched" situation [13]. In addition, the SPs exist as an evanescent wave and hence can exponentially decay along the depth [18]. Therefore, the dielectric media surrounding the top and bottom side of the Al film should be effectively uniform within the penetration depth of SP resonance in order to obtain the matched SP modes [19]. In the PF, the LiF overlayer provides an effective dielectric constant at the top interface, similar to that of the bottom interface. Further, it also works as a protective layer against metal oxidation.

The optical structure of the PF was designed by numerical simulation using a finite-difference time domain method (FDTD Solutions, Lumerical Inc., Canada). In the numerical method, a unit cell, as illustrated in Fig. 1(a), was simulated with boundary conditions of symmetry and anti-symmetry in the x and y directions, respectively. For the boundary in the z direction, a perfect matching layer condition was set. The dielectric constants of Al and SiO_2 were obtained from Palik data [20], while that of LiF was obtained from experimental data [21]. The dimensions of the reference structure are as follows – 350 nm P (period of hole array), 75 nm T_{Al} (thickness of the Al layer), 150 nm T_{LiF} (thickness of the LiF overlayer), and 130 nm D (diameter of holes).

Fig. 1(b) represents the calculated transmission spectrum of the optimized PF for red color. The maximum transmittance peak appears at 642 nm with 10.4% transmittance intensity and a full width at half maximum (FWHM) of 54 nm. As expected from (1), optical resonance has multiple orders in accordance with the reciprocal order of the periodic domain. Therefore, the transmission spectrum has additional small peaks at 575 nm (2.8%) and 485 nm (5.5%).

The transmittance peak at $\lambda_{max(1,0)}$ corresponding to 624 nm in this case is not symmetrical in the spectral region. The range of FWHM is divided by 19 nm on the left side and 35 nm on the right side. Surface plasmon resonance is affected by the optical constants of the dielectric and metal at the interface (as expected from (1)). It is also affected by geometrical factors. The left minimum wavelength of $\lambda_{max(1,0)}$ is affected by a periodic geometry (Wood's anomaly) [22]. The tail-like shape on the right side of the peak is related to the life time of SPs [22]. The high uniformity of the hole patterns results in a longer life time for SPs and finally a faster decay on the right side of the peak. This will be analyzed for the

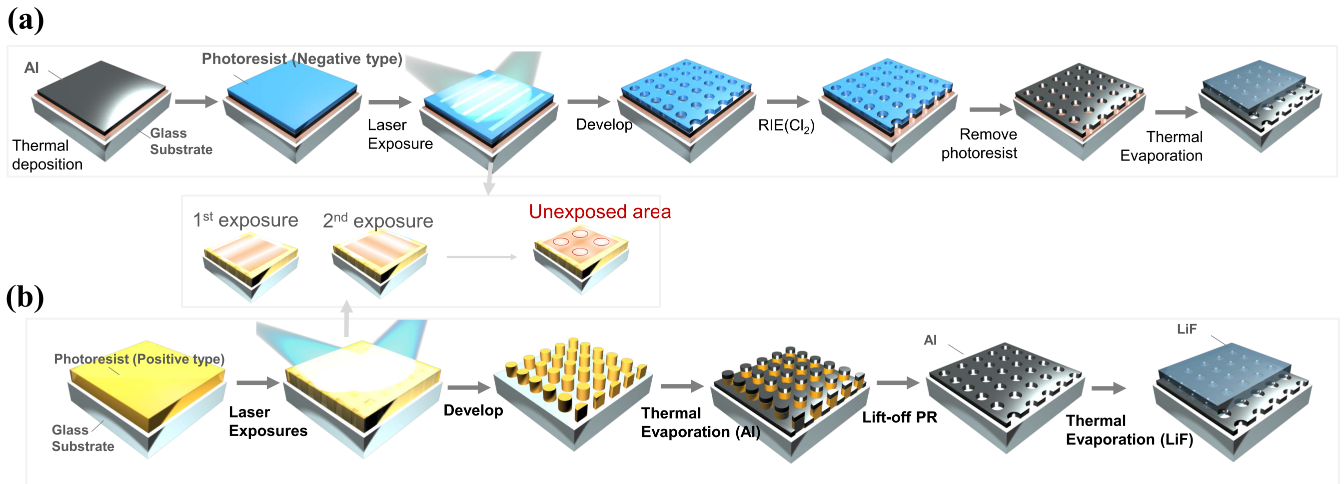

FIGURE 2. Schematic diagram of the fabrication process of plasmonic filters. During the lithography process with a Lloyd's mirror interferometer system, exposure was conducted twice in the horizontal and vertical directions. Each process includes a photoresist layer with (a) a negative photoresist and (b) a positive photoresist.

fabricated samples in a later section for analyzing the quality of the patterning produced using the direct method.

III. FABRICATION PROCESS WITH HIGH REPRODUCIBILITY

A. FABRICATION PROCESS OF PLASMONIC FILTERS

To fabricate 2D square hole arrays, the LIL method was employed. The interference pattern of two coherent beams results in a periodically sinusoidal one-dimensional intensity profile. The photoresist (PR) layer is exposed to the interference patterns in both horizontal and vertical directions. At this point, the PR layer can be distinguished by the difference between the area exposed at least once and the unexposed area. The beam power was controlled along with the exposure time of the interfered beams in order to separate these two areas. As the laser beam has a high spatial coherence, LIL yields perfect periodicity over large areas. Therefore, the LIL fabrication of plasmonic color filters is an easy method to achieve high-performance large-size PFs using simple maskless equipment.

Fig. 2 illustrates the whole fabrication process of PFs (including LIL). Fig. 2(a) depicts the method we proposed in a previous study [13]. On a glass substrate of 2.5 cm × 2.5 cm, a LiF buffer layer, Al layer, and PR layer were deposited. Subsequently, LIL was performed. In this case, the PR was negative and hence the obtained pattern contained shapes in the form of holes. The PR layer undergoing LIL works as a masking layer during reactive ion etching (RIE) of the Al layer.

The regular periodicity obtained using the process in Fig. 2 across the entire area resulted in a good accordance between the spectral position of maximum transmittance and the simulation. However, the poor uniformity of hole patterns led to a degraded selective filtering performance. In addition, RIE, a quasi-isotropic etching methods, provided another factor to make poor uniformity. The etch-rate of Al is hardly maintained stable. Therefore, successive RIE under a LIL-processed PR layer might degrade the accuracy of patterning; in addition, the etched holes are not perfectly cylindrical. This process showed low reproducibility in the RIE step.

Fig. 2(b) shows a modified process in order to reduce the degradation in the filtering performance originating from the etching step (Method b). In contrast to the previous case, the PR material was positive, which allows reversal of the hole patterns, i.e., nano dot arrays. Instead of etching, the patterned PR layer works as a template during Al deposition. Firstly, after conducting LIL on a glass substrate, a 75-nm thick Al layer was deposited by thermal evaporation. In particular, there were no rotations of the substrate holders during thermal evaporation. This was advantageous for the next step, as the PR pillars could be removed more efficiently. After lifting off the PR layer with acetone, a 150-nm thick LiF overlayer was deposited by thermal evaporation for matching SP modes at the top and bottom and protecting the metal layer from oxidation.

The LiF buffer layer of the structure in Fig. 2(a) was removed in the modified process shown in Fig. 2(b). The thermally evaporated LiF medium adhered weakly to the additionally deposited Al layer on top. In thermal evaporation technology, generally, pre-deposition of a small amount of chromium (Cr) or titanium (Ti) can enhance adhesion between a substrate and the evaporated majority material. When a LiF buffer layer, which is a good adhesive to the substrate and weak adhesive to the Al upper layer, was used in "Method b," the Al film and PR pattern lifted off simultaneously. In the case of the previously suggested process, RIE provided a physical pressure vertically pressing down and that helps to combine the PR and the Al layer at the bottom. Adversely, this could cause residual PR particle formation after RIE. In order to avoid both PR residue and weak adhesion, the buffer layer was removed. As explained earlier,

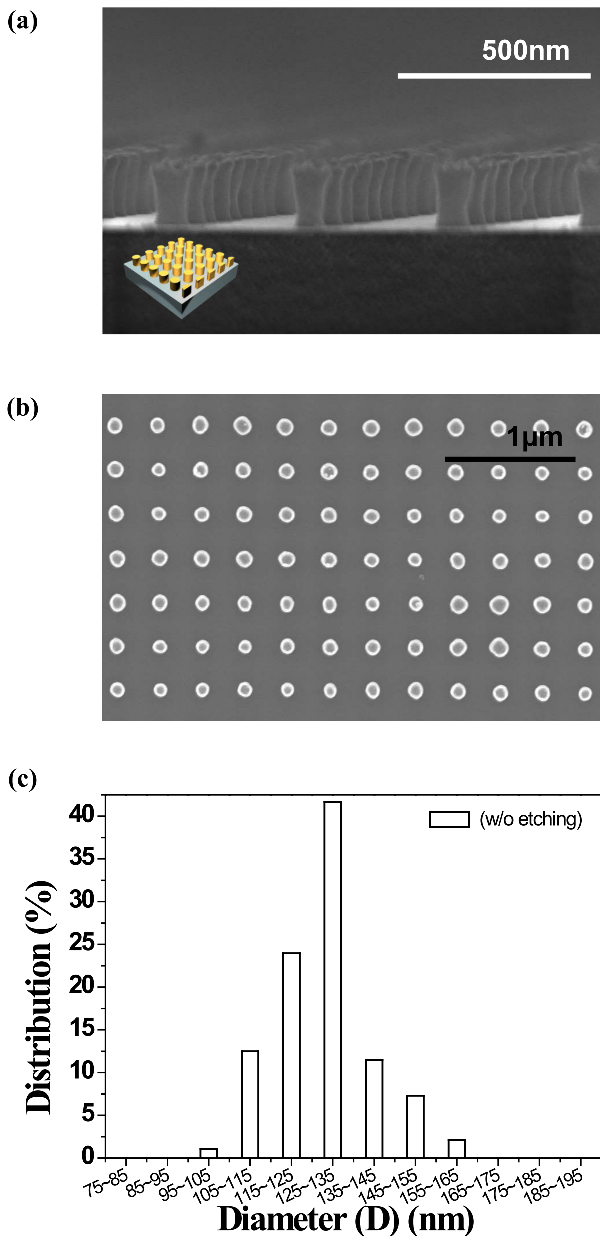

FIGURE 3. Scanning electron microscope (SEM) images of the dot-array patterns in the photoresist layer. (a) Cross section and (b) top surface of the photoresist layer. The size distribution of the holes in (b) is analyzed as described in the histogram in (c).

matched SP modes between the top and bottom sides of the Al film can be obtained within the effective dimensions as the SPs exist in an evanescent field. For the buffer layer between the substrate and Al film, materials which can be handled by coating technologies with hard or soft baking could be considered.

B. THE FARICATED PLASMONIC FILTER AND ITS OPTICAL CHARACTERISTICS

A PF-R structure was fabricated using ''Method b.'' Fig. 3(a) and 3(b) show scanning electron microscope images of the fabricated sample after the LIL process. Cylinder-like pillars can be observed at a regular periodicity. The pillars are not shaped in an ideal cylindrical form because the interference beam profile is also sinusoidal in the direction of penetration into the PR layer. The top surface has the biggest diameter and hence it is possible to separate the PR pillars from the deposited Al layer at the substrate surface. Since the distance between the evaporation source and the target sample in the equipment is short enough that the evaporated Al is deposited in the vertical direction. Therefore, the lift-off step becomes more efficient. And finally the shape of the holes in the Al layer well follows the shape of the top surface of the pillars.

The modified process, in particular, provided higher accuracy with respect to the metallic hole patterns. The diameter of the top surface of each pillar is directly related to the size of the holes in the Al film. An analysis of pattern uniformity in terms of the size of the dots is shown in Fig. 3(b); the distribution diagram is represented in Fig. 3(c). The size of the dot patterns was divided by 10 nm for comparing with the data in a previous study, which employed ''Method b'' with RIE. Removing the RIE step resulted in an enhancement in the pattern accuracy. Compared to the previous study, the targeted pattern size, within a ± 5 nm error, improved from 33.1% to 41.7%. The largest error was 35 nm, while that of the process with RIE was 63 nm. Further, the trend of the hole patterns seems more Gaussian.

In addition, ''Method b'' led to better stability and a higher reproducibility of patterning across a large fabrication area. The area of the interfered beam profile had a circular shape with a diameter of 5.3 cm. The sample of 2.5 cm $\times$ 2.5 cm square area was aligned at the center of the interfered beam. Therefore, both the samples fabricated with ''Method a'' and ''Method b'' showed a uniformly constant color across the whole area. (More data on size distribution of different points are included in the supplementary material, Fig. S1) However, imperfections in the fabrication process produced patterning errors at the micrometer scale that could not be detected by the naked eye.

The fabricated samples are represented in Fig.4. Fig. 4(c) and 4(d) show microscopic images obtained with a transmission configuration (DM2000, Leica, Germany). In the case of ''Method a,'' failure of the hole patterns originated from over-etching of the Al film. The photoresist layer damaged during the RIE step as well as the non-flat surfaces cannot be etched evenly across the entire area. As a result, the surfaces of the substrate are revealed randomly as shown in Fig. 4(c). On the other hand, the defects resulting from ''Method b'' were residuals of the PR pillars. The areas where the PR materials were not removed, but were covered with Al, forming lightly protruding spots instead of holes, and the defect morphology can generate scattering. This resulted in greenish gray points, as represented in Fig. 4(d). The sizes of these defects are much smaller than those of the defects produced in ''Method a.''

The defects of each sample affected the spectral response, as shown in Fig. 5. The transmittance spectra of the fabricated

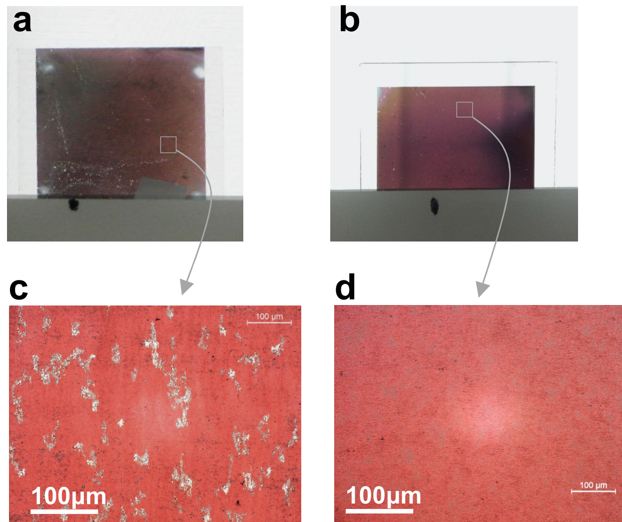

FIGURE 4. Photographs and optical microscope images of the fabricated PFs. (a) and (c) PF-R fabricated using a process including the RIE technique, "Method a." (b) and (d) PF-R fabricated the modified fabrication process, "Method b."

PF-Rs were measured with a spectrophotometer (UV-2550, Shimadzu, Japan). Imperfections in the fabrication process resulted in a degradation in the filtering characteristics in both cases, i.e., lowering of the transmission intensity and peak broadening.

The sample processed by "Method a" showed a 9.6% maximum transmittance at 631 nm corresponding to the $\lambda_{max(1,0)}$ peak. Higher order peaks appeared at 527 nm (4.5%) and 430 nm (5.3%). The maximum transmittance of the sample processed by "Method b" was 7.63% at 649 nm and the sample exhibited smaller additional peaks as well; one peak with 0.59% transmittance at 563 nm and a broad peak ranging from 420 nm to 550 nm with 2.71% maximum transmittance.

The size distributions of the holes and defects (in tens of micrometers), as shown in Fig. 4, can shorten the life time of the SPs and consequently lead to peak broadening. The left side of the FWHM was similar in both cases – 49 nm for "Method a" and 42 nm for "Method b." However, "Method b" resulted in a wider range on the right side of the FWHM (155 nm as compared to 141 nm for "Method a"). As LIL results in a regular periodicity across the entire fabrication area, the left minimum wavelength of $\lambda_{max(1,0)}$ could be affected in a similar manner in both the samples.

The right side of the peak, which is a result of the life time of SPs, is affected by the defect regions at the micrometer scale. The sample processed by "Method b" includes a continuous Al film with a protruding morphology in the defect regions. As the spots are aligned with a 350-nm period, it also works as a scattering source. It could disturb SP resonance from the holes resulting in a shortening in the life time of the SPs. Meanwhile, "Method a" doesn't include any metallic patterns. Although the surface morphology of the defect regions is slightly bumpy, the randomness and refractive index of LiF result in a weak scattering and other photonic effects. Instead, light can simply pass through the defect region.

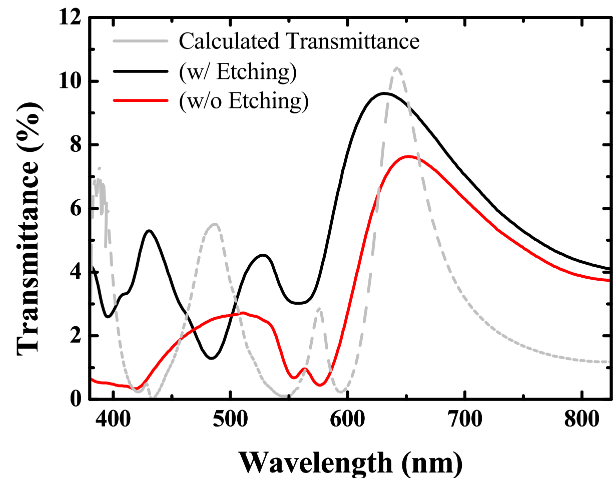

FIGURE 5. Transmission spectra of the fabricated plasmonic filters. Dry etching method (black solid line) and without a dry etching method (red solid line). The calculated transmittance curve (gray dotted line) is represented for a comparison between the simulated and experimental results.

Finally, "Method b" is advantageous to demonstrate an optically stable filter. The process without etching resulted in a broader peak as compared to that of the sample undergoing etching. However, light directly passes through the over-etched region and finally the spectrum has an offset value in the entire spectral region, as shown in Fig. 5. Although the maximum transmittance value is similar to the calculated value, its value is originated from the offset and consequently this degrades the color purity as well as the selective filtering performance. In addition, the sample fabricated using "Method b" showed good agreement with the simulation in terms of peak positions.

IV. DISCUSSION

PF-Rs showed around 10% maximum transmittance even in simulations. This is not enough for use in imaging devices, such as displays. The shape of holes and T_{Al} affect to the maximum transmittance value. The size and shape of holes are related to the localized quantity of each SP resonance modes which occurs at top and bottom surface of the Al film (SP_{top} and SP_{bottom}), respectively [4]. And a thin metal layer help SP modes (SP_{top} and SP_{bottom}) to be coupled to each other and finally to result in high transmittance [23]. These phenomena are caused by the relative size. The spectral change according to D is evaluated and summarized in the Supplementary material. (Fig. S2 and Table S1) The opening ratio of holes with 130 nm D is 10.8% while the maximum transmittance of PF resulted in 10.4%. Compared to 150 nm T_{Al}, the hole shape is closer to deep than shallow. In the deep hole regime, the coupling opportunity between SP modes is reduced. Thus the maximum transmittance of the designed PF-R could not exceed in the opening ratio. On the other

hand, D becomes larger than T_{Al}, EOT results in the higher transmittance than the opening ratio.

This study is focused on verification of the fabrication in terms of realization. So a PF-R has been designed, whose structure consists of tiny nano holes. With LIL, a design of nano apertures sized in less than half of P is a hard condition to realize. Since the PR pillars became thinner toward the bottom, smaller diameter of the pillars have more possibilities of defects providing absence of the pillars when over-exposed or over-etched.

Although LIL has a limitation that it can only fabricate simple periodic patterns, it is an attractive additional solution for conventional methods for large area applications in which periodic patterns are desirable [24]–[27]. Compared to directly writing patterning methods such as electron beam lithography or focused ion beam, LIL requires much shorter process time. In our experiment, a circular area with 5.3 cm of diameter was exposed for 140 s. The high accuracy of the periodicity originated from the coherence of the laser beam source results in good accordance with the designed spectral peak positions. And this work provides more precise guide to manipulate LIL for fabricating PFs under poor pattern uniformity. Additionally, one pixel of the PFs can be reduced to 1 μm [28] and the interference pattern with a period of hundreds of nanometers is small enough to separate the patterned area in pixel units. Thus, it is possible to generate spatial separation of colors by shadow masking and multiple exposures.

LiF was chosen as the material for the buffer layer after considering the in-situ process of the whole structure. Finally it was removed in ''Method b'' due to weak adhesion. However, it might be possible to insert several coated layers, which is a more realistic design for integration with conventional emitting devices.

The broadened shape and spectral shift of the peaks can be attributed to the non-uniformity in hole patterns. The hole size distribution is associated with the uniformity of the absorbed energy in the PR layer during exposure. Thus the pattern uniformity was maintained at a similar level regardless of the dimension. Since the interference beam has a submicron scaled profile, light scattering by small particles or weak vibration of air could interrupt the exposure uniformity. Our experimental setup for conducting LIL did not have any equipment to control the disturbance. By controlling dusts and vibrations in the air, the pattern uniformity could be improved. Although both samples showed degradation in their optical characteristics, the spectral response affected by the defects generated in ''Method b'' is more suitable for a selective filtering device.

V. CONCLUSION

In this study, large-area plasmonic color filters with high reproducibility are demonstrated. Because the fabricated hole array showed high accuracy and good periodic regularity, the pass band corresponds well with the calculated results. Although poor uniformity in the hole size results in a low transmission and broad bandwidth, the results indicate a high feasibility for the fabricated PFs for application in industrial devices. In addition, the modified fabrication process without the RIE step allowed better reproducibility of metallic hole patterns. It is expected that these results will provide an opportunity to converge diverse nanotechnological disciplines for mass production and advanced optical devices.

ACKNOWLEDGMENT

Y. S. Do thanks K. C. Choi, B. K. Ju, and their research groups for helping with material fabrication and in-depth discussion.

REFERENCES

[1] T. W. Ebbesen, H. J. Lezec, H. F. Ghaemi, P. A. Wolff, and T. Thio, ''Extraordinary optical transmission through sub-wavelength hole arrays,'' *Nature*, vol. 391, pp. 667–669, Feb. 1988.
[2] J. Li *et al.*, ''Dependence of surface plasmon lifetimes on the hole size in two-dimensional metallic arrays,'' *Appl. Phys. Lett.*, vol. 94, p. 183112, May 2009.
[3] L. Martín-Moreno *et al.*, ''Theory of extraordinary optical transmission through subwavelength hole arrays,'' *Phys. Rev. Lett.*, vol. 86, no. 6, pp. 1114–1117, 2001.
[4] A. Degiron, H. J. Lezec, W. L. Barnes, and T. W. Ebbesen, ''Effects of hole depth on enhanced light transmission through subwavelength hole arrays,'' *Appl. Phys. Lett.*, vol. 81, pp. 4327–4329, Nov. 2002.
[5] C. Genet and T. W. Ebbesen, ''Light in tiny holes,'' *Nature*, vol. 445, no. 7123, pp. 39–46, Jan. 2007.
[6] H. A. Bethe, ''Theory of diffraction by small holes,'' *Phys. Rev. Lett.*, vol. 66, nos. 7–8, pp. 163–182, Oct. 1944.
[7] Q. Chen and D. R. S. Cumming, ''High transmission and low color cross-talk plasmonic color filters using triangular-lattice hole arrays in aluminum films,'' *Opt. Express*, vol. 18, no. 13, pp. 14056–14062, Jun. 2010.
[8] K. A. Tetz, L. Pang, and Y. Fainman, ''High-resolution surface plasmon resonance sensor based on linewidth-optimized nanohole array transmittance,'' *Opt. Lett.*, vol. 31, no. 10, pp. 1528–1530, May 2006.
[9] S. Lal, S. Link, and N. J. Halas, ''Nano-optics from sensing to waveguiding,'' *Nature Photon.*, vol. 1, pp. 641–648, Nov. 2007.
[10] K. A. Willets and R. P. Van Duyne, ''Localized surface plasmon resonance spectroscopy and sensing,'' *Annu. Rev. Phys. Chem.*, vol. 58, pp. 267–297, May 2007.
[11] Y. S. Do and K. C. Choi, ''Matching surface plasmon modes in symmetry-broken structures for nanohole-based color filter,'' *IEEE Photo. Technol. Lett.*, vol. 25, no. 24, pp. 2454–2457, Dec. 2013.
[12] Y. S. Do and K. C. Choi, ''Poly-periodic hole arrays for angle-invariant plasmonic filters,'' *Opt. Lett.*, vol. 40, no. 16, pp. 3873–3876, Aug. 2015.
[13] Y. S. Do, J.-H. Park, B. Y. Hwang, S.-M. Lee, B.-K. Ju, and K. C. Choi, ''Plasmonic color filter and its fabrication for large-area applications,'' *Adv. Opt. Mater.*, vol. 1, no. 2, pp. 133–138, Feb. 2013.
[14] S. Chang *et al.*, ''Photo-insensitive amorphous oxide thin-film transistor integrated with a plasmonic filter for transparent electronics,'' *Adv. Funct. Mater*, vol. 24, no. 23, pp. 3482–3487, Jun. 2014.
[15] Y.-G. Moon *et al.*, ''Plasmonic chromatic electrode with low resistivity,'' *Sci. Rep.*, vol. 7, Nov. 2017, Art. no. 15206.
[16] C. Genet, M. P. van Exter, and J. P. Woerdman, ''Fano-type interpretation of red shifts and red tails in hole array transmission spectra,'' *Opt. Commun.*, vol. 225, nos. 4–6, pp. 331–336, Oct. 2003.
[17] S.-H. Chang, S. K. Gray, and G. C. Schatz, ''Surface plasmon generation and light transmission by isolated nanoholes and arrays of nanoholes in thin metal films,'' *Opt. Express*, vol. 13, no. 8, pp. 3150–3165, Apr. 2005.
[18] W. L. Barnes, ''Surface plasmon–polariton length scales: A route to sub-wavelength optics,'' *J. Opt. A, Pure Appl. Opt.*, vol. 8, no. 4, pp. S87–S93, Mar. 2006.
[19] Y. S. Do and K. C. Choi, ''Quantitative analysis of enhancing extraordinary optical transmission affected by dielectric environment,'' *J. Opt.*, vol. 16, no. 6, pp. 065005-1–065005-5, May 2014.
[20] E. D. Palik, *Handbook of Optical Constants of Solids*. San Diego, CA, USA: Academic, 1998.
[21] R. M. Montereali, A. Mancini, G. C. Righini, and S. Pelli, ''Active stripe waveguides produced by electron beam lithography in LiF single crystals,'' *Opt. Commun.*, vol. 153, pp. 223–225, Aug. 1998.

[22] H. F. Ghaemi, T. Thio, D. E. Grupp, T. W. Ebbesen, and H. J. Lezec, ''Surface plasmons enhance optical transmission through subwavelength holes,'' *Phys. Rev. B, Condens. Matter*, vol. 58, nos. 11–15, p. 6779, Sep. 1998.

[23] K. L. van der Molen, F. B. Segerink, N. F. van Hulst, and L. Kuipers, ''Influence of hole size on the extraordinary transmission through subwavelength hole arrays,'' *Appl. Phys. Lett.*, vol. 85, no. 19, pp. 4316–4318, Nov. 2004.

[24] L. E. Gutierrez-Rivera and L. Cescato, ''SU-8 submicrometric sieves recorded by UV interference lithography,'' *J. Micromech. Microeng.*, vol. 18., no. 11, p. 115003, Sep. 2008.

[25] Q. Xie, M. H. Hong, H. L. Tan, G. X. Chen, L. P. Shi, and T. C. Chong, ''Fabrication of nanostructures with laser interference lithography,'' *J. Alloys Compounds*, vol. 449, nos. 1–2, pp. 261–264, Jan. 2008.

[26] J. de Boor, D. S. Kim, and V. Schmidt, ''Sub-50 nm patterning by immersion interference lithography using a Littrow prism as a lloyd's interferometer,'' *Opt. Lett.*, vol. 35, no. 20, pp. 3450–3452, Nov. 2010.

[27] R. Murillo, H. A. van Wolferen, L. Abelmann, and J. C. Lodder, ''Fabrication of patterned magnetic nanodots by laser interference lithography,'' *Microelectron. Eng.*, vols. 78–79, pp. 260–265, Mar. 2005.

[28] S. Yokogawa, S. P. Burgos, and H. A. Atwater, ''Plasmonic color filters for CMOS image sensor applications,'' *Nano Lett.*, vol. 12, no. 8, pp. 4349–4354, Jul. 2012.

YUN SEON DO was born in Daegu, South Korea, in 1983. She received the B.S. degree in electrical engineering from Kyungpook National University, Daegu, in 2005, and the M.S. and Ph.D. degrees in electrical engineering from KAIST, Daejeon, South Korea, in 2007 and 2013, respectively.

From 2007 to 2009, she was a Researcher with the Daegu Gyeongbook Institute of Science Technology. She was a Senior Research Engineer with the Department of Frontier Technology, Samsung Display, from 2013 to 2017. She is currently an Assistant Professor with the School of Electronics Engineering, Kyungpook National University. Her research interests include plasmonics, novel nanophotonic physics, active nanophotonic devices, and electrical applications of such nanostructures for light emitting devices and solar energy devices, flexible and transparent displays, and light sensors (gas, bio, and robots).

Dr. Do received the Outstanding Poster Paper Award from the International Display Workshops in 2006 and the Annual Honor Prize from the Department of Electrical Engineering, KAIST, in 2013. One of her research papers was selected as the Best of Advanced Optical Materials 2013.